JOURNAL OF CLINICAL MICROBIOLOGY, Apr. 2011, p. 1411–1420 Vol. 49, No. 4
0095-1137/11/$12.00 doi:10.1128/JCM.00756-10

Adenoid Reservoir for Pathogenic Biofilm Bacteria▽

L. Nistico,[1] R. Kreft,[1] A. Gieseke,[2] J. M. Coticchia,[3] A. Burrows,[4] P. Khampang,[4] Y. Liu,[5] J. E. Kerschner,[4] J. C. Post,[1,5] S. Lonergan,[6]† R. Sampath,[6] F. Z. Hu,[1,5] G. D. Ehrlich,[1,5] P. Stoodley,[1,5,7] and L. Hall-Stoodley[1,5,8]*

Center for Genomic Sciences, Allegheny-Singer Research Institute, Allegheny General Hospital, Pittsburgh, Pennsylvania[1]; Max-Planck Institute for Marine Microbiology, Bremen, Germany[2]; Wayne State University, Detroit, Michigan[3]; Medical College of Wisconsin, Milwaukee, Wisconsin[4]; Drexel University College of Medicine, Allegheny Campus, Pittsburgh, Pennsylvania[5]; Ibis Division, Isis Corp., Carlsbad, California[6]; University of Southampton, National Centre for Advanced Tribology, School of Engineering Sciences, Southampton, United Kingdom[7]; and University of Southampton, Infection, Inflammation and Immunity Division, Faculty of Medicine, NIHR Respiratory BRU and Wellcome Trust Clinical Research Facility, Southampton, United Kingdom[8]

Received 14 April 2010/Returned for modification 27 August 2010/Accepted 1 February 2011

Biofilms of pathogenic bacteria are present on the middle ear mucosa of children with chronic otitis media (COM) and may contribute to the persistence of pathogens and the recalcitrance of COM to antibiotic treatment. Controlled studies indicate that adenoidectomy is effective in the treatment of COM, suggesting that the adenoids may act as a reservoir for COM pathogens. To investigate the bacterial community in the adenoid, samples were obtained from 35 children undergoing adenoidectomy for chronic OM or obstructive sleep apnea. We used a novel, culture-independent molecular diagnostic methodology, followed by confocal microscopy, to investigate the *in situ* distribution and organization of pathogens in the adenoids to determine whether pathogenic bacteria exhibited criteria characteristic of biofilms. The Ibis T5000 Universal Biosensor System was used to interrogate the extent of the microbial diversity within adenoid biopsy specimens. Using a suite of 16 broad-range bacterial primers, we demonstrated that adenoids from both diagnostic groups were colonized with polymicrobial biofilms. *Haemophilus influenzae* was present in more adenoids from the COM group ($P = 0.005$), but there was no significant difference between the two patient groups for *Streptococcus pneumoniae* or *Staphylococcus aureus*. Fluorescence *in situ* hybridization, lectin binding, and the use of antibodies specific for host epithelial cells demonstrated that pathogens were aggregated, surrounded by a carbohydrate matrix, and localized on and within the epithelial cell surface, which is consistent with criteria for bacterial biofilms.

Chronic otitis media (COM) is a primary reason for young children to visit a physician. An early childhood history of COM can result in auditory and verbal disabilities that exert influence into late childhood, rendering treatment of recurrent otitis media (ROM) and otitis media with effusion (OME) desirable (2, 4, 5, 6, 67). Repeated cycles of antibiotics for treatment of COM make it the leading reason for antibiotic usage in children (2). Treatment may also entail surgery for the placement of tympanostomy tubes (TT) to reduce the incidence of ROM and alleviate middle ear fluid associated with OME. Adenoidectomy has been shown to be an effective treatment for COM in randomized controlled studies and, together with TT placement, has been associated with reduced need of further surgical intervention for OM (15, 25, 26, 37). Adenoidectomy is also performed for the treatment of obstructive sleep apnea (OSA) and as an adjunctive therapy for patients suffering from chronic rhinosinusitis (CRS) (44). Several reports have examined the bacteria present in adenoids from these diagnostic groups using culture-based methods and shown that adenoids harbor bacteria (9, 10, 16, 21, 62, 68). Adenoidectomy may also remove a physical obstruction of the Eustachian tubes, thereby restoring mucus drainage and normal pressure in the middle ear (7) affecting the ability of pathogens to invade and reside within the middle ear space. However, adenoidectomy is effective for reducing the recurrence of COM regardless of the size of adenoids in children >3 years of age, suggesting that physical obstruction of the airway may not be the principal risk factor in COM (26, 49). While OM is certainly a multifactorial disease, it is now well established that viral infection of the upper respiratory tract (URT) is a predisposing risk that influences the ability of bacterial pathogens prevalent in OM, such as *Haemophilus influenzae*, *Streptococcus pneumoniae*, and *Moraxella catarrhalis*, which normally colonize the nasopharynx, to induce inflammation and invasion of the middle ear mucosa (MEM) (5). Thus, adenoidectomy is thought to remove a reservoir of pathogens that transiently colonize the URT mucosal epithelium and contribute to this polymicrobial infection.

A current hypothesis suggests that COM is associated with the persistence of bacterial pathogens in biofilms despite the use of antibiotics. This hypothesis has been supported by both animal model studies in experimentally infected chinchillas (20, 36, 58) and a prospective clinical trial in which bacterial biofilms of *H. influenzae*, *S. pneumoniae*, and *M. catarrhalis*

* Corresponding author. Mailing address: University of Southampton Wellcome Trust Clinical Research Facility, Mailpoint 218, C Level, West Wing, Southampton General Hospital, Tremona Rd., Southampton SO16 6YD, United Kingdom. Phone: 44 (0)2380 794989. Fax: 44 (0)2380 795023. E-mail: l.hall-stoodley@soton.ac.uk.

† Present address: Nerites Corp., 525 Science Dr., Ste. 215, Madison, WI 53711.

▽ Published ahead of print on 9 February 2011.

were directly detected on the MEM epithelia obtained from children undergoing TT placement for the treatment of COM (28). No evidence of OM pathogens was found on the MEM of uninfected animals or in humans in a control population without a history of OM undergoing surgery for the placement of cochlear implants, suggesting that pathogenic biofilms are not present on the MEM in the absence of middle-ear disease.

Moreover, several studies describe biofilms consisting of unidentified bacteria on the surfaces and crypts of adenoids removed from children being treated for COM, CRS, chronic adenotonsillitis, and OSA and within the tissue and crypts of inflamed tonsils from children with chronic tonsillitis (1, 11, 38, 55), demonstrating that uncharacterized bacterial biofilms are present in other chronic URT infections. Biofilm infections are clinically significant because these three-dimensional (3D), adherent, organized communities of bacteria are far more recalcitrant to antibiotic therapy and killing by host phagocytic cells (27, 30, 35).

Few clinical studies, however, have documented the presence of specific bacterial pathogens that meet the criteria for biofilm infections. These criteria are as follows: (i) bacteria are aggregated, (ii) bacteria are associated with a surface (epithelium), (iii) bacteria are encased in a complex extracellular matrix, and (iv) bacteria are recalcitrant to antibiotic treatment (30, 52). Although simple diagnostic methods are currently lacking for determining that an infection is biofilm associated, it is nevertheless possible to assess which pathogens are present and how pathogens are distributed and organized in clinical specimens and whether the criteria for biofilm infections are met (28, 42). The *in situ* demonstration of bacterial pathogens in biofilms on a mucosal surface in the respiratory tract during different disease states will improve our understanding of the various strategies used by microorganisms to persist in the face of intact host immune responses and antibiotic therapy in chronic infections (50). Furthermore, a better understanding of the complex polymicrobial-host interactions that play a role in COM will better facilitate the design of more effective clinical treatments.

We undertook the present study to assess whether there were (i) differences in the bacterial population in the adenoids between two pediatric diagnostic groups undergoing adenoidectomy for either COM or OSA and (ii) whether pathogenic bacteria were present in biofilms which might contribute to the persistence of pathogens in the URT. For the first objective, we used a novel, culture-independent approach, the Ibis T5000 system, which detects and identifies the presence of a broad range of bacteria (17, 18, 19). We used this approach because culture-independent techniques have proved superior in detecting bacteria associated with chronic inflammatory infections such as COM (28, 53, 57). However, while conventional PCR requires the *a priori* choice of pathogen-specific primers and probes to target bacteria that may be present, the Ibis T5000 uses mass spectrometry-derived base composition microbial signatures obtained from the PCR amplification of multiple, widely conserved genes (including a combination of 16S ribosomal DNA and selected housekeeping gene primers) present in the sample to yield species-specific bacterial resolution regardless of species or phylogeny. We further investigated the adenoid tissue of the two diagnostic groups *in situ* using confocal laser scanning microscopy (CLSM) to evaluate whether selected bacterial pathogens associated with adenoids met specific criteria for biofilm infections using fluorescence *in situ* hybridization (FISH), carbohydrate probes, and antibodies specific for epithelial cells.

MATERIALS AND METHODS

Patient population. Adenoids were obtained from 35 children between 1 and 10 years of age (mean age, 4.1 years; 18 males and 17 females), undergoing routine adenoidectomy for either COM ($n = 23$) or OSA ($n = 12$). Patients were enrolled in the Division of Pediatric Otolaryngology, Wayne State University School of Medicine, Detroit, Michigan, and in the Division of Pediatric Otolaryngology, Department of Otolaryngology and Communication Sciences, Medical College of Wisconsin, Milwaukee, Wisconsin, with IRB approval from both institutions.

Adenoid tissue acquisition and preparation. Immediately after surgery the specimens were either placed in sterile Hanks buffered saline solution (HBSS) (Invitrogen, Carlsbad, CA) or snap-frozen in liquid nitrogen and shipped overnight on ice or dry ice, respectively, to the Center for Genomic Sciences (CGS). On arrival at the CGS, Ibis samples (12 COM and 10 OSA) were stored at −80°C until evaluation with the Ibis T5000 biosensor system. Adenoids for *in situ* analysis (12 COM and 6 OSA) were immediately immersed in fresh, sterile HBSS, and one section of the tissue was used immediately to assess bacteria viability, extracellular matrix presence and antibiotic susceptibility, while the remaining part of the specimen was fixed with fresh 4% paraformaldehyde (Electron Microscopy Sciences, Hatfield, PA) in 3× phosphate-buffered saline (PBS) overnight at 4°C. Fixed samples were then washed with PBS and stored in 1:1 PBS-ethanol at −20°C until evaluation with FISH, generic fluorescent staining, and immunostaining.

Ibis T5000 biosensor system evaluation of adenoid tissue. Nucleic acid (NA) was extracted from the samples according to standard Qiagen protocols (Qiagen, Germantown, MD). Briefly, 25 mg of tissue was teased apart in ATL (lysis) buffer and added to 100 μl of 0.1-mm zirconia/silica beads (19). Separately, 200 μl of medium was added to 500 μl of ATL buffer and 100 μl of beads and then processed for 20 min in a Qiagen tissue lyser. Two hundred microliters of material was placed in a mini-spin column and washed to yield 200 μl of purified genomic material, 5 μl of which was added to each well of a broad screening TAR 35 lower-calibrant-level (low Cal) plate. Six samples were run per plate and 45 PCR cycles were performed, followed by desalting for electron spray ionization (ESI) and time-of-flight (TOF) mass spectrometric (MS) analysis.

CLSM. CSLM imaging was performed as described previously (51). Briefly, after staining, tissues were mounted in a 35-mm petri plate and imaged with a Leica DM RXE microscope attached to a TCS SP2 AOBS confocal system (Leica Microsystems, Exton, PA) using either a ×63 water immersion lens (NA 1.2) or a ×10 dry objective lens for low-power mapping. Sequential scanning was used to further eliminate interference from multiple dyes. Images were collected and analyzed by using the Leica LCS software and Imaris software (Bitplane, St. Paul, MN) by one observer who was blinded to the diagnostic group to which the adenoids belonged.

In situ viability and antibiotic susceptibility assays. Fresh adenoidal tissue was rinsed with sterile HBSS, sectioned into approximately 0.25- to 0.5-cm-thick sections with a sterile surgical scalpel and stained with BacLight Live/Dead NA probes (Invitrogen) according to the manufacturer's instructions to stain live bacteria green and dead bacteria red. A subset of fresh tissue sections was assayed to determine *in situ* antibiotic killing. Briefly, 2 mg of azithromycin (USP, Rockport, MD)/ml in sterile HBSS was added to some adenoid sections, followed by incubation for 2 h at 37°C (43). Azithromycin was selected because (i) it is widely used in infections of the middle ear and oropharynx and (ii) it accumulates in macrophages and in tracheal epithelial fetal cell lines (43). For this reason, it should broadly kill both extracellular and intracellular bacteria. Although we could not determine the MIC of the bacteria present in the tissue, since MIC is measured on planktonic cells, we know from Thornsberry et al. (64) that the MIC_{90} for *H. influenzae* is 2 μg/ml (1,032 isolates tested), that for *S. pneumoniae* is 16 μg/ml (1,275 isolates tested), and that for *M. catarrhalis* is 0.12 μg/ml (444 isolates tested). However, bacteria in biofilms are often over 100 times more resistant to antibiotics (14, 23, 29, 65). We therefore used 2 mg/ml because it is >125 times the MIC_{90} of the most common respiratory pathogens and should sufficiently test whether biofilm bacteria demonstrated increased recalcitrance to antibiotic. One tissue section in each experiment was incubated with HBSS alone without antibiotic. Sections were then rinsed, stained with the BacLight Live/Dead, and imaged by using CLSM, as previously described (51).

FISH. FISH was performed on a subset of 18 adenoids (12 OM and 6 OSA) as previously described (28, 51). Briefly, fixed adenoids were sectioned as described above, and a solution of 0.5 mg of lysozyme (Sigma)/ml in 0.1 M Tris-HCl and 0.05 M Na_2EDTA was added to the specimens, followed by incubation at 37°C for 3 h as an additional permeabilization step for the improved detection of Gram-positive bacteria. Fixed, permeabilized adenoid sections were then incubated in an ethanol series of 80 and 100% for 3 min each, and FISH was performed with species-specific and genus-specific fluorescent 16S rRNA probes for *H. influenzae*, *S. pneumoniae*, *M. catarrhalis*, *Staphylococcus aureus*, *Streptococcus* sp., and *Staphylococcus* sp. (Integrated DNA Technologies, Inc, Coralville, IA), conjugated with FAM-5 or the sulfoindocyanine dyes Cy3 or Cy5. All FISH probes used in the present study were extensively tested for cross-reactivity for respiratory pathogens (28). The "universal" eubacterial (EUB338) and nonsense (NONEUB338) probes were used as positive and negative controls and hybridization conditions were tested systematically *in vitro* to ensure specificity for each probe. Each adenoid section was incubated with probe-specific formamide and salt concentrations and then immersed in washing buffer with the probe-specific salt concentration as previously described (28, 51). Samples were rinsed in sterile MilliQ water and observed with CLSM.

Quantitative analysis of bacteria in tissue sections. The total number of bacteria in each adenoid tissue section (six sections per adenoid) was quantified by counting the number of adherent bacterial cells and bacterial cells within biofilm aggregates in 10 random fields of view using Imaris image analysis software. Bacterial aggregates and individual cells that would otherwise be obscured in a flat projection were readily discernible by rendering the confocal stacks and three-dimensionally rotating the image.

Bacterial localization and immunostaining. To determine the distribution of bacteria specifically associated with adenoid tissue, adenoid tissue was stained with phalloidin, a general eukaryotic cytoskeletal stain specific for filamentous actin (F-actin), and the cytokeratin 5/6/8/18 mouse monoclonal antibody cocktail, which was used as a marker for epithelial cells. For F-actin staining, tissue samples were first treated with 0.1% Triton in HBSS for 3 to 5 min to permeabilize the adenoidal epithelial cells, rinsed, and stained with Alexa Fluor 488-phalloidin (Invitrogen) for 25 min. Samples were simultaneously stained with Syto 59 (Invitrogen) according to the manufacturer's instructions to generally stain bacteria and to visualize host cell nuclei. For cytokeratin immunostaining of epithelial cells, an antigen retrieval protocol was used for specimens previously fixed for FISH. Briefly, samples were rinsed with sterile HBSS and blocked with 5% fetal bovine serum (FBS; HyClone, Logan, UT) for 30 min, rinsed again with HBSS, and incubated with 2.1 mg of citric acid (Fisher Scientific)/ml in double-distilled water (pH 3) for 1 h at 37°C. After a rinse with HBSS–5% FBS, the samples were incubated with cytokeratin 5/6/8/18 mouse monoclonal antibody cocktail (Vector Laboratories, Burlingame, CA) at 1:50 in HBSS for 1 h at 37°C, washed with HBSS–5% FBS, and incubated with 20 μg of anti-mouse fluorescein-conjugated IgG (Vector Laboratories, Burlingame, CA)/ml for 1 h. Samples were rinsed, stained with Syto 59, and imaged by using CLSM.

Lectin binding to extrapolymeric carbohydrates. A subset of fresh sections of adenoid tissue was also stained with a cocktail of Alexa 488-conjugated lectins (Invitrogen) specific for α-mannopyranosyl, α-glucopyranosyl, and terminal α- and β-linked *N*-acetyl-D-glucosaminyl, β-galactose and α- and β-*N*-acetyl-galactosamine and galactopyranosyl residues to assess the presence of the polysaccharide components as evidence of a biofilm EPS (29). Then, 3 μl of Syto 59 NA stain was added per ml of cocktail to stain the bacteria and host nuclei. Samples were stained for 35 min, rinsed to remove unbound probes, and examined with CLSM.

Statistics. Data were reported as means ± 1 standard deviation (SD). Statistical comparisons were made by using one-way analysis of variance (Excel, Microsoft Office 2003). Differences were considered statistically significant for $P < 0.05$.

RESULTS

Initial identification of bacteria using Ibis T5000 analysis. *H. influenzae*, *S. pneumoniae*, *M. catarrhalis*, and *S. aureus* were present in 66.7, 50, 16.6, and 8.3%, respectively, of adenoids obtained from patients with a history of COM (Table 1). In contrast, these same organisms were found in 10, 50, 10, and 30%, respectively, of adenoids from patients with OSA. The pathogen makeup of the COM and OSA diagnostic groups (measured as present or absent) differed significantly only for *H. influenzae* ($P = 0.005$). Although there was no statistical difference between the two patient groups for the presence of *S. pneumoniae*, the frequency of nonpneumococcal streptococci, including hemolytic and viridans streptococcal species, was greater in the COM group ($P < 0.005$). In addition to the three major OM pathogens and *S. aureus*, Ibis T5000 broad-based analyses demonstrated the presence of a number of other oral and upper respiratory tract pathogens, including pathogenic streptococci, *Pseudomonas aeruginosa*, *Neisseria meningitidis*, and others (Table 1). The anaerobe *Fusobacterium nucleatum* was found in 17% of adenoids from children with COM and in 40% of adenoids from OSA patients. *S. aureus* was three times more likely to be in adenoids from patients with OSA than from COM patients; however there was no statistically significant difference between these two groups ($P > 0.05$). The bacterial diversity was twice as great for adenoids from the COM group, with 24 different types of bacteria present, compared to 10 in the OSA group.

TABLE 1. Bacteria detected by using the Ibis T5000 Biosensor in adenoids from children with COM and OSA

Organism	No. (%) of isolates	
	COM ($n = 12$)	OSA ($n = 10$)
Aerobic and facultative organisms		
Gram-positive cocci		
Streptococcus pneumoniae	6 (50)	5 (50)
Staphylococcus aureus	1 (8.3)	3 (30)
Staphylococcus hominis	1 (8.3)	0 (0)
Hemolytic and viridans streptococci		
Streptococcus thermophilus	2 (16.6)	0 (0)
Streptococcus gordonii	2 (16.6)	0 (0)
Other *Streptococcus* spp.		
Streptococcus mitis or *S. agalactiae*	1 (8.3)	1 (10)
Streptococcus mutans, *S. peroris*, or *S. anginosus*	1 (8.3)	0 (0)
Streptococcus/Enterococcus	1 (8.3)	0 (0)
Gram-negative cocci		
Moraxella catarrhalis	2 (16.6)	1 (10)
Neisseria meningitidis	1 (8.3)	0 (0)
Neisseria flavescens	1 (8.3)	0 (0)
Gram-positive bacilli		
Corynebacterium pseudodiphtheriticum	1 (8.3)	0 (0)
Arthrobacter oxydans	1 (8.3)	0 (0)
Gram-negative bacilli		
Haemophilus influenzae[a]	8 (66.7)	1 (10)
Pseudomonas aeruginosa	1 (8.3)	0 (0)
Serratia marcescens	1 (8.3)	0 (0)
Mannheimia haemolytica	1 (8.3)	0 (0)
Moraxella sp.	1 (8.3)	2 (20)
Mannheimia, *Pasteurella*, and *Haemophilus* spp.	0 (0)	1 (10)
Enterobacter sp.	1 (9.1)	0 (0)
Microaerophilic and anaerobic organisms		
Gram-positive bacilli		
Eubacterium sulci	1 (8.3)	0 (0)
Gram-negative bacilli		
Fusobacterium nucleatum	2 (16.6)	4 (40)
Prevotella intermedia	0 (0)	1 (10)
Prevotella spp.	0 (0)	1 (10)
Total [pathogen/adenoid ratio]	24/12 [2.0]	10 [1]

[a] $P = 0.005$.

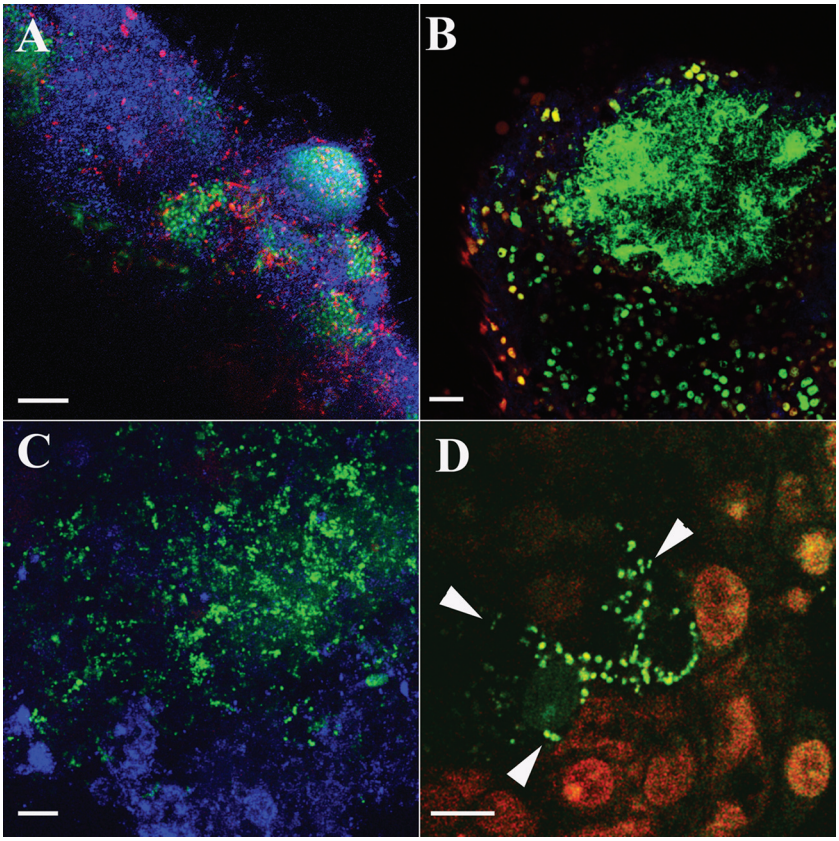

FIG. 1. Viable bacteria on adenoids from four patients undergoing adenoidectomy for treatment of COM. (A) Live (green) and dead (red) bacteria adherent to the adenoid mucosal surface. (B) Aggregated live bacteria covering ~100 μm on the adenoid surface treated with azithromycin. (C) Viable single-celled and bacterial clusters (green) adherent to the mucosal surface stained with phalloidin (blue). (D) Viable bacteria within a crypt showing diplococci (arrowheads). Scale bar, 10 μm.

***In situ* determination of pathogen distribution and ultrastructure.** Unfixed adenoid samples were examined *in situ* upon receipt using the BacLight viability stain, which demonstrated viable bacteria associated with the epithelial surfaces of adenoids in all samples. Moreover, many of the bacteria associated with the mucosal surface were present as large aggregates (Fig. 1). Both cocci and rods covered the adenoidal epithelial surface, with numerous single cells and bacterial aggregates attached to the mucosal surface. The distribution was heterogeneous with some areas of the mucosa associated with multiple layers of bacteria, while other areas were devoid of bacteria. Furthermore, *in situ* antibiotic susceptibility assays performed on a subset of the adenoid samples showed that there were viable bacteria present even after treatment with >100 times the MIC_{90} of azithromycin for 2 h. Figure 1B shows representative images from three replicate experiments.

FISH-based analyses demonstrated that pathogenic bacteria were present on and within the adenoids from both COM and OSA patient groups. Bacterial aggregates were associated with the surface of the adenoid adherent to the epithelium, within crypts, and intracellularly (Fig. 2). The pathogens *H. influenzae*, *S. pneumoniae*, *M. catarrhalis*, and *S. aureus* were all observed associated with the surface epithelium, and some of these were also observed intracellularly, adjacent to the host cell nucleus in several samples (Fig. 2D). PCR confirmed the presence of *H. influenzae* in 11 of 12 FISH-positive COM samples and the presence of *S. pneumoniae* in 10 of 11 FISH-positive COM adenoids (>90% correlation). PCR also confirmed in one case the absence of *S. pneumoniae* in a FISH-negative COM sample.

***In situ* quantitative assessment of pathogenic bacteria.** COM adenoids exhibited 50 and 70% more *H. influenzae* and *M. catarrhalis* bacteria, respectively, than adenoids from OSA patients, and *H. influenzae* cell clusters were present twice as often in COM adenoids compared to OSA adenoids. However, these differences were not significant ($P > 0.05$) (Fig. 2I). Both diagnostic groups showed similar numbers of *S. pneumoniae* and *S. aureus*. The COM patient group had 3.4 times more *Streptococcus* sp. associated with adenoid tissues compared to the OSA group; however, this was not statistically significant (data not shown).

Lectin binding and colocalization with bacterial carbohydrate matrix in adenoids. Since bacterial viability staining on fresh adenoids and 16S FISH both demonstrated that bacteria were found in aggregates, we further examined these bacterial aggregates to determine whether they exhibited a carbohydrate matrix, which is a hallmark of biofilm (Fig. 3). The colocalization of lectin and NA probes demonstrated that carbohydrate binding occurred only in the presence of bacteria that stained with the Syto 59 NA probe. Thus, bacteria were observed

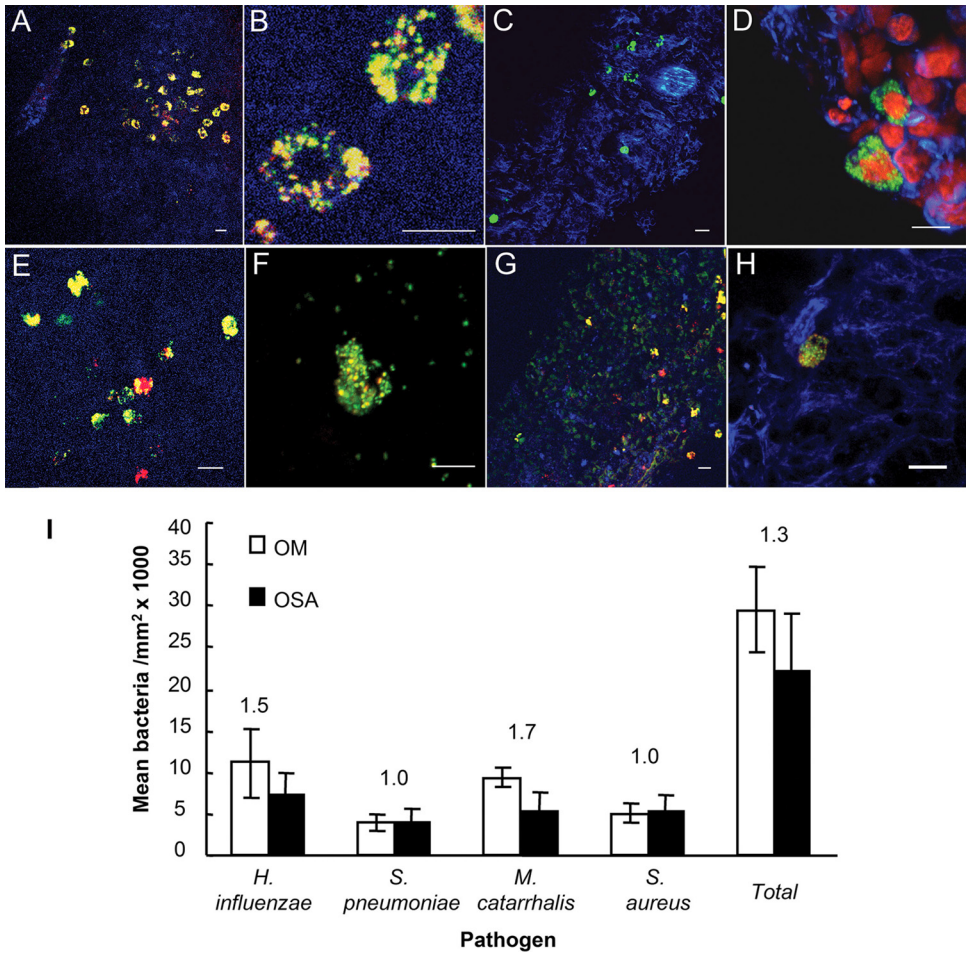

FIG. 2. *In situ* pathogen distribution and organization in adenoid tissue. (A and B) *H. influenzae*-specific (green) and EUB (red) 16S rRNA probes, hybridizing with bacterial clusters in an adenoid crypt from a child with COM (A) and, at higher magnification, coccobacillus morphology (B). (C and D) *S. pneumoniae*-specific probe (green) on phalloidin-stained adenoid cells (blue) from a child undergoing adenoidectomy for OSA (C) and a higher-magnification image of aggregated *S. pneumoniae* (green) surrounded by host cell cytoskeleton (blue) and nuclei (red) (D). (E and F) *M. catarrhalis* (green) in a COM adenoid and unidentified bacteria hybridized with the universal eubacterial probe (red). (G and H) Bacteria hybridized with *S. aureus* (green) and eubacterial (red) probes in an OSA adenoid. Scale bar, 10 μm. (I) Mean number of bacteria/mm^2 identified by FISH in adenoid tissue sections from COM or OSA groups. The numbers above the bars represent the pathogen ratio: COM versus OSA. Error bars, 1 SD.

directly attached to the mucosal surface and encased in an extracellular polymeric substance (EPS) matrix characteristic of bacterial biofilms, in this case a carbohydrate matrix. Intracellular pathogenic bacteria were also enveloped within an EPS matrix evidenced by carbohydrate binding within the epithelial cells (Fig. 4).

Localization of bacteria adjacent to and within adenoidal epithelial cells. Phalloidin labeling of F-actin to determine the localization of bacterial cells relative to host tissue was inconclusive since phalloidin stains F-actin in multiple cell types. Therefore, immunostaining with an epithelial cell specific antibody cocktail was used to determine whether bacteria were specifically associated with adenoidal epithelial cells. When FISH was followed by immunostaining with a pan-cytokeratin monoclonal antibody cocktail, bacterial aggregates were observed attached to the mucosal epithelial surface and localized within the epithelial cell cytoplasm (Fig. 5). Intracellular aggregates were determined to be inside epithelial cells by (i) the lack of polymorphous lobed nuclei, readily observed after nucleic acid staining, and (ii) positive immunostaining with the pan-cytokeratin-specific antibody. Intracellular bacteria were densely packed together and brightly fluorescent, a finding consistent with the presence of high numbers of ribosomes (22). The bacteria were observed adjacent to the nuclei within the cytoplasm of epithelial cells. Intracellular *S. pneumoniae* was present in adenoids from both groups.

DISCUSSION

To test clinically relevant specimens for the presence of pathogenic biofilms, we examined adenoidal tissue from children undergoing adenoidectomy for COM or OSA using molecular and *in situ* imaging approaches to see whether these clinical diagnoses differed in (i) the types of pathogens associated with the adenoids and (ii) the distribution of pathogenic species in adenoid tissue. The Ibis T5000 Universal Biosensor

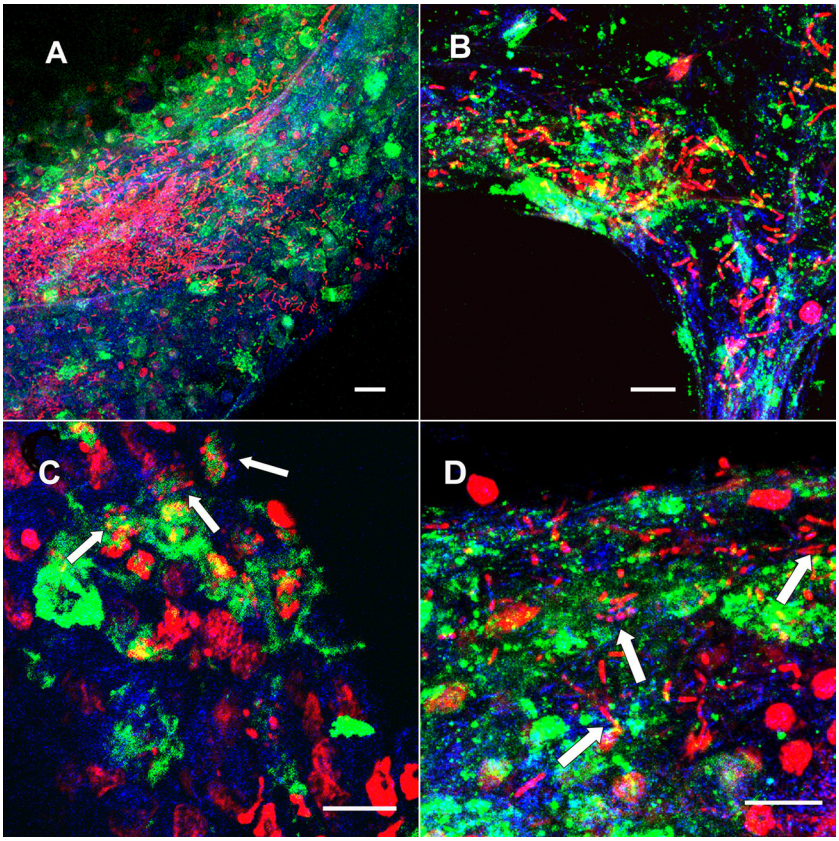

FIG. 3. Bacteria on adenoid mucosa from patients with COM exhibit a carbohydrate matrix. (A) Rods and cocci stained with Syto 59 (red) (which also stains host nuclei) overlying adenoid tissue (blue) colocalized with lectin, which binds carbohydrates (green). (B) Panel A at a higher magnification. (C and D) Higher-resolution images showing cocci and rods (arrows) surrounded by lectin-bound matrix (green). The blue is the reflected light from the tissue. Scale bar, 10 μm.

has advantages over conventional PCR detection methods because it does not require a presumptive target and detects a broad range of bacteria more rapidly compared to culture methods (17–19, 35), making it a powerful tool for determining the presence of bacteria in a clinical sample. The Ibis approach indicated that multiple aerobic and anaerobic bacteria were present in the adenoids of both the COM and the OSA diagnostic groups (Table 1) with differences between the two groups. First, *H. influenzae* was more frequently detected in the COM group than in the OSA diagnostic group ($P = 0.005$). Second, there was twice the species diversity of bacteria present in adenoids from the COM group, including several pathogens associated with other diseases of the human oronasopharynx, than in the OSA group. Third, there was no statistical difference between the two patient groups for the presence of *S. pneumoniae*; however, the frequency of nonpneumococcal streptococci, including hemolytic and viridans streptococcal species, was greater in the COM group in accordance with the increased microbial diversity present in this group. *F. nucleatum* was present in adenoids from both OSA and COM. This anaerobic bacterium is believed to contribute to the coaggregation of polymicrobial oral bacteria, leading to biofilm formation in plaque and periodontal disease (39), and others have identified this pathogen in the NP of patients with OM (32) and in adenoids using anaerobic culture methodology (10, 11).

The localization and distribution of bacteria associated with adenoids was investigated using several *in situ* methods designed to assess whether bacteria met several specific criteria for biofilms. Extensive mucosal biofilms, indicated by large aggregates of viable bacteria, and attached to the adenoidal surface epithelium were observed using CLSM in conjunction with BacLight NA or lectin probes on unfixed tissue, followed by CLSM with FISH probes on fixed tissue. Concomitant FISH and lectin probe staining demonstrated that carbohydrate colocalized specifically with *H. influenzae*, *S. pneumoniae*, *M. catarrhalis*, and *S. aureus.* 3D structures encased in an extracellular matrix and associated with the epithelia indicate that a carbohydrate matrix bound by the lectin probes is produced by bacteria. Although the biofilm matrix is structurally complex (29, 34, 36), demonstration of the matrix with carbohydrate probes gave the most unambiguous results of intracellular biofilms. Furthermore, *ex vivo* incubation of the adenoid epithelium with antibiotics demonstrated that biofilm bacteria were recalcitrant to antibiotic killing.

H. influenzae, *S. pneumoniae*, *M. catarrhalis*, and *S. aureus* were present in adenoids from both diagnostic groups in biofilm clusters localized on the mucosal surface and within adenoid crypts. Moreover, FISH and CLSM better demonstrated that pathogen-specific bacteria were present in aggregated 3D structures in tissue samples compared to conventional thin-

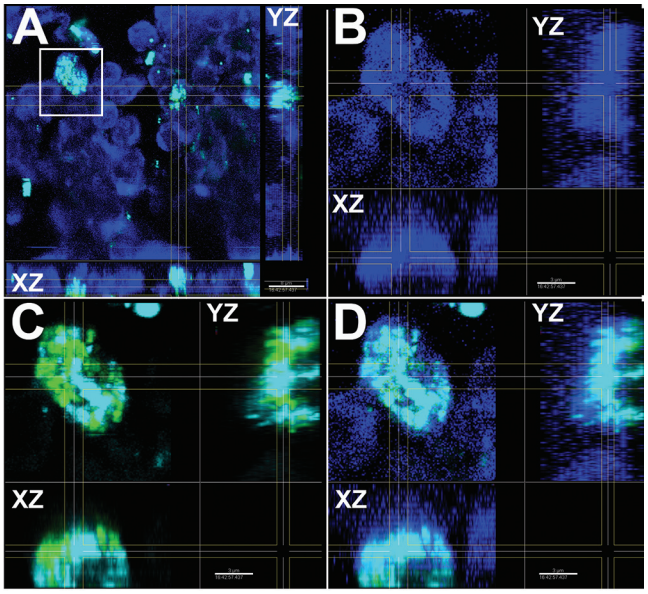

FIG. 4. Intracellular bacteria exhibit an EPS matrix characteristic of biofilms. (A) Low-power magnification shows epithelial cells (blue) and 16S hybridized bacteria (green). Scale bar, 8 μm. (B) High power of invaded cell stained with epithelial cell-specific monoclonal antibody (blue) alone. (C) Same region showing EUB338$^+$ bacteria (green) with EPS (cyan) colocalized with lectin probes. (D) Overlay of panels B and C. Cross-sections show bacteria within the epithelial cell. Scale bar, 3 μm. The subpanels show a *xy* plan view with *xz* and *yz* sagittal sections, below and to the right, respectively.

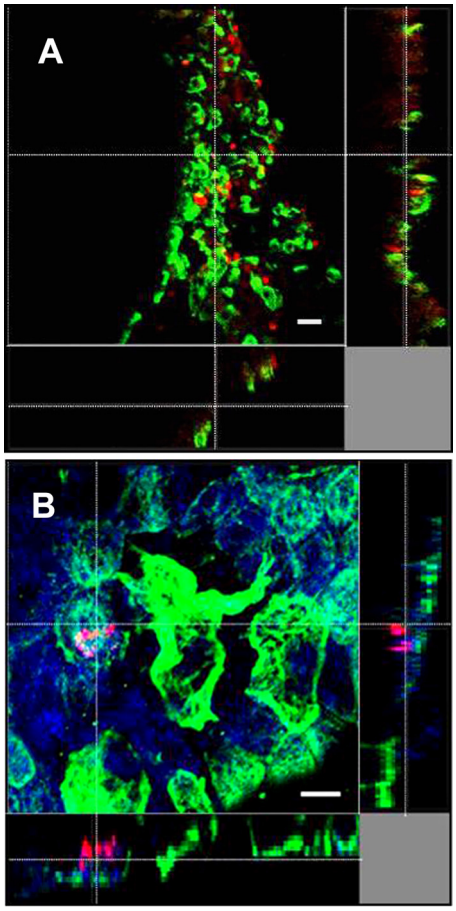

FIG. 5. Intracellular pathogens within adenoids stained with an antibody specific for epithelial cells. Epithelial cells (green) with intracellular *S. pneumoniae* (A) and EUB338 plus bacteria (B), hybridized with 16S FISH probes (red). Blue is the reflected light from the tissue. Cross-sections show bacteria within the epithelial cell. Scale bar, 10 μm. The subpanels show a *xy* plan view, with *xz* and *yz* sagittal sections, below and to the right, respectively.

section hematoxylin-and-eosin staining of the same tissue (data not shown). We have previously used FISH to evaluate multiple clinical tissues for bacterial biofilms in clinical infections where the etiology of infection is unknown (40, 51, 61), with similar qualitative results.

To attempt to quantify the frequency of different bacteria by another method, we used FISH in conjunction with 3D image analysis. The results indicated that the ratio of *H. influenzae* in cell clusters was greater in adenoids from COM compared to OSA; however, the Ibis approach alone showed a significant difference in the frequency of *H. influenzae* between the two groups. These results are broadly consistent with other researchers who have reported the presence of *H. influenzae* in pediatric adenoids using culture. Suzuki et al. showed that adenoids from children with OME had significantly more *H. influenzae* than adenoids from children without OME (62). In that study, the authors also noted an increased likelihood of patients with OME to have rhinosinusitis. Faden et al. also showed that the carriage rate of *H. influenzae* was greater in young children with OME, and the extent of colonization correlated with OME (21).

Forsgren et al. (22), however, found no significant difference in *H. influenzae* in children with or without OME using FISH 16S rRNA probes. FISH is extremely sensitive, and Heiniger et al. found it had the highest detection rate of *M. catarrhalis* in clinical samples, exhibiting a higher rate than surface culture, PCR, or immunohistochemistry (33). Although our results using quantitative FISH analysis supported the trend of more *H. influenzae* in COM, it did not show significant differences between the patient groups. This may be because CLSM/FISH quantitative image analysis was labor-intensive and therefore possibly more prone to sampling error. The Ibis approach, on the other hand, detected pathogens in a completely nonanticipatory and nonbiased way using the amplicon weight to calculate a base composition signature, which is then checked against a database of >300 phylogenetically diverse bacteria (18). These results suggest that Ibis was superior for quantitative detection, while FISH was better suited for confirming the presence of specific pathogens and determining whether they met specific criteria for biofilms in clinical samples.

Nevertheless, quantitative image analyses of OM-specific pathogenic bacteria in adenoid samples using FISH probes, broadly supported Ibis results. *S. pneumoniae* and *S. aureus* were present in similar ratios in adenoids from both COM and OSA groups, and the frequency of cell clusters hybridizing with the *Streptococcus* genus 16S FISH probe was 2-fold higher in adenoids from COM than from OSA, also supporting Ibis analysis. Colonization of the NP with *S. pneumoniae* and *S. aureus* is common and dependent upon age and daycare attendance (8). The finding that *S. aureus* was present in adenoids is

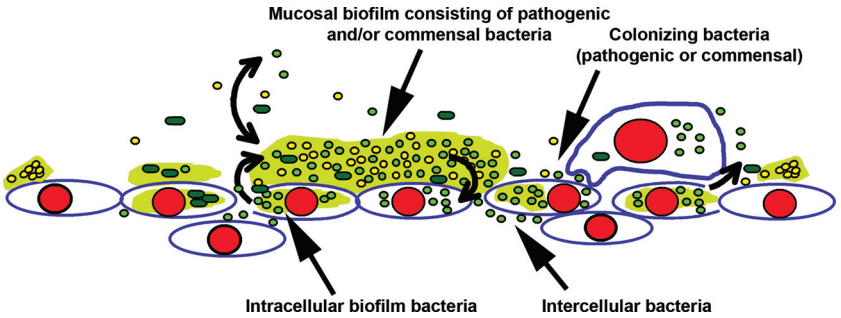

FIG. 6. Schematic showing bacteria, as observed in adenoids in biofilm aggregates on the epithelial surface and within epithelial cells. Biofilm bacteria may include phenotypes that adhere to and invade the cell. Both extracellular and intracellular biofilms would protect against phagocytosis. Although infected epithelial cells may be sloughed off, pathogenic bacteria would be released by cell lysis to initiate further rounds of attachment and invasion.

consistent with the clinical observation that adenoidectomy improves signs and symptoms associated with CRS in children (48). Overall, these data suggest that hypertrophic adenoids, removed for OSA, are infected with pneumococcus and/or *S. aureus*, a result that invites further study.

To further investigate the specific localization of bacteria in biofilms on adenoid tissue, FISH was used in combination with the fluorescently conjugated cell markers, phalloidin and pankeratin. Pathogenic biofilms colocalized with host cells in adenoid tissue stained with phalloidin, frequently appearing to be inside the cytoplasm, and we hypothesized that the extensive rinsing associated with FISH increased the likelihood of finding intracellular pathogens. However, since phagocytic cells also contain F-actin, particularly following bacterial induced motility (47), pathogenic biofilms were further assayed for their specific association with the adenoid epithelium using an antibody specific for epithelial cells. These experiments demonstrated that bacteria were associated specifically with epithelial cells, sometimes located intracellularly. Intracellular 3D structures of *H. influenzae*, *S. pneumoniae*, *M. catarrhalis*, and *S. aureus*, as with extracellular biofilms were encased in a carbohydrate matrix, indicating that intracellular aggregates were biofilms (Fig. 4).

Numerous reports have demonstrated these pathogens adhere to and invade epithelial cells. *H. influenzae* utilizes several adhesive factors which lead to colonization and invasion of human epithelial cells, including adenoidal epithelium (44, 54, 55, 63). Specifically, adhesins, pili, and lipooligosaccharides associated with *H. influenzae* lead to the attachment and invasion of cultured human epithelial cells via diverse pathways (41, 60, 63). *M. catarrhalis* has been shown to colonize and invade pharyngeal epithelial cells (45, 59), and intracellular *M. catarrhalis* was specifically found in adenoids and tonsils (33). Intracellular *S. aureus* was demonstrated in nasal epithelium from patients treated for CRS (12, 62). *S. pneumoniae* has been shown to invade broncho-epithelial cells (54) and appears to modulate capsule production upon adherence to epithelium (31) and during pneumococcal biofilm formation *in vitro* (29). Intracellular pneumococcus has also been demonstrated *in vivo* in the MEM of children with OME (13). Intracellular biofilm development has been observed in respiratory epithelial cells with *Pseudomonas aeruginosa* (24), where biofilm clusters in airway epithelial cells were resistant to antibiotic killing.

It is possible that polymicrobial interactions between *H. influenzae* and *S. pneumoniae* may facilitate the invasion of epithelial cells. Ratner et al. have shown that peptidoglycan from *H. influenzae* synergizes with pneumococcal pneumolysin resulting in the invasion of epithelial cells by *H. influenzae* (56) and coinfection with *H. influenzae* resulted in the selection of a more invasive *S. pneumoniae* strain (46). These and other data suggest that the host response, as well as competitive interactions between colonizing microorganisms, influence the outcome of the host response and the elimination or persistence of bacteria. Polymicrobial interactions also appear to affect biofilm development by OM pathogens. Coinfection studies with NTHi in the chinchilla model of OM indicated that NTHi facilitated biofilm formation by *S. pneumoniae* (66) and *M. catarrhalis* (3).

Biofilm development may influence the expression of surface molecules that facilitate bacterial adherence and invasion (Fig. 6) in response to selection pressures found in the human upper respiratory tract such as antibiotic exposure, host immune responses, and polymicrobial interactions. Our data show that the principal OM pathogens, as well as *S. aureus*, are present in biofilms on the adenoid surface *in vivo* associated with human disease (COM) and in OSA according to at least four specific criteria. Our results also indicate that the microbial complexity of the human respiratory tract in COM may be currently underestimated (5, 50). The Ibis approach in conjunction with FISH may therefore present a significant advance in the investigation of the complexity in biofilm-associated diseases in general and COM in particular.

ACKNOWLEDGMENTS

This study was supported by Allegheny General Hospital/Allegheny Singer Research Institute and grants from the National Institute on Deafness and Other Communication Disorders: DC05659 (J.C.P.), DC04173 (G.D.E.), and DC02148 (G.D.E.).

We thank Mary O'Toole, Center for Genomic Sciences, Allegheny-Singer Research Institute, for help in the preparation of the manuscript.

REFERENCES

1. **Al-Mazrou, K. A., and A. S. Al-Khattaf.** 2008. Adherent biofilms in adenotonsillar diseases in children. Arch. Otolaryngol. Head Neck Surg. **134:**20–23.
2. **American Academy of Family Physicians/American Academy of Otolaryngology-Head and Neck Surgery/American Academy of Pediatrics Subcom-**

mittee on Otitis Media with Effusion. 2004. Otitis media with effusion. Pediatrics **113:**1412–1429.
3. **Armbruster, C. E., et al.** 2010. Indirect Pathogenicity of *Haemophilus influenzae* and *Moraxella catarrhalis* in polymicrobial otitis media occurs via interspecies quorum signaling. MBio **1:**e00102–e00110.
4. **Bakaletz, L. O.** 2002. Otitis media, p. 259–298. *In* K. A. Brogden and J. M. Guthmiller (ed.), Polymicrobial diseases. ASM Press, Washington, DC.
5. **Bakaletz, L. O.** 2010. Immunopathogenesis of polymicrobial otitis media. J. Leukoc. Biol. **87:**213–222.
6. **Bennett, K. E., M. P. Haggard, P. A. Silva, and I. A. Stewart.** 2001. Behavior and developmental effects of otitis media with effusion into the teens. Arch. Dis. Child. **85:**91–95.
7. **Bluestone, C. D.** 1996. Pathogenesis of otitis media: role of Eustachian tube. Pediatr. Infect. Dis. J. **15:**281–291.
8. **Bogaert, D., et al.** 2004. Colonisation by *Streptococcus pneumoniae* and *Staphylococcus aureus* in healthy children. Lancet **363:**1871–1872.
9. **Brook, I., K. Shah, and W. Jackson.** 2000. Microbiology of healthy and diseased adenoids. Laryngoscope **110:**994–999.
10. **Brook, I., and K. Shah.** 2001. Bacteriology of adenoids and tonsils in children with recurrent adenotonsillitis. Ann. Otol. Rhinol. Laryngol. **110:**844–848.
11. **Chole, R. A., and B. T. Faddis.** 2003. Anatomical evidence of microbial biofilms in tonsillar tissues: a possible mechanism to explain chronicity. Arch. Otolaryngol. Head Neck Surg. **129:**634–636.
12. **Clement, S., et al.** 2005. Evidence of an intracellular reservoir in the nasal mucosa of patients with recurrent *Staphylococcus aureus* rhinosinusitis. J. Infect. Dis. **92:**1023–1028.
13. **Coates, H., et al.** 2008. The role of chronic infection in children with otitis media with effusion: evidence for intracellular persistence of bacteria. Otolaryngol. Head Neck Surg. **138:**778–781.
14. **Costerton, J. W., P. S. Stewart, and E. P. Greenberg.** 1999. Bacterial biofilms: a common cause of persistent infections. Science **284:**1318–1322.
15. **Coyte, P. C., R. Croxford, W. McIsaac, W. Feldman, and J. Friedberg.** 2001. The role of adjuvant adenoidectomy and tonsillectomy in the outcome of the insertion of tympanostomy tubes. N. Engl. J. Med. **344:**1188–1195.
16. **DeDio, R. M., et al.** 1988. Microbiology of the tonsils and adenoids in a pediatric population. Arch. Otolaryngol. Head Neck Surg. **114:**763–765.
17. **Ecker, D. J., et al.** 2008. Ibis T5000: a universal biosensor approach for microbiology. Nat. Rev. Microbiol. **6:**553–558.
18. **Ecker, D. J., et al.** 2010. New Technology for rapid molecular diagnosis of bloodstream infections. Expert Rev. Mol. Diagn. **10:**399–415.
19. **Ecker, D. J., et al.** 2005. Rapid identification and strain-typing of respiratory pathogens for epidemic surveillance. Proc. Natl. Acad. Sci. U. S. A. **102:**8012–8017.
20. **Ehrlich, G. D., et al.** 2002. Mucosal biofilm formation in middle-ear mucosa in the chinchilla model of otitis media. JAMA **287:**1710–1715.
21. **Faden, H., et al.** 1991. Nasopharyngeal flora in the first three years of life in normal and otitis-prone children. Ann. Otol. Rhinol. Laryngol. **100:**612–615.
22. **Forsgren, J., et al.** 1994. *Haemophilus influenzae* resides and multiplies intracellularly in human adenoid tissue as demonstrated by in situ hybridization and bacterial viability assay. Infect. Immun. **62:**673–679.
23. **Fux, C. A., S. Wilson, and P. Stoodley.** 2004. Detachment characteristics and oxacillin resistance of *Staphylococcus aureus* biofilm emboli in an *in vitro* catheter infection model. J. Bacteriol. **186:**4486–4491.
24. **Garcia-Medina, R. W. M. Dunne, P. K. Singh, and S. L. Brody.** 2005. *Pseudomonas aeruginosa* acquired biofilm-like properties within airway epithelial cells. Infect. Immun. **73:**8298–8305.
25. **Gates, G. A., C. A. Avery, T. J. Prihoda, and J. C. Cooper, Jr.** 1987. Effectiveness of adenoidectomy and tympanostomy tubes in the treatment of chronic otitis media with effusion. N. Engl. J. Med. **317:**1444–1451.
26. **Gates, G. A.** 1999. Otitis media: the pharyngeal connection. JAMA **282:**987–989.
27. **Hall-Stoodley, L., J. W. Costerton, and P. Stoodley.** 2004. Bacterial biofilms: from the natural environment to infectious diseases. Nat. Rev. Microbiol. **2:**95–108.
28. **Hall-Stoodley, L., et al.** 2006. Direct detection of bacterial biofilms on the middle-ear mucosa of children with chronic otitis media. JAMA **296:**202–211.
29. **Hall-Stoodley, L., et al.** 2008. Characterization of biofilm matrix, degradation by DNase treatment and evidence of capsule downregulation in *Streptococcus pneumoniae* clinical isolates. BMC Microbiol. **8:**173.
30. **Hall-Stoodley, L., and P. Stoodley.** 2009. Evolving concepts in biofilm infections: microreview on modeling pathogenesis. Cell Microbiol. **11:**1034.
31. **Hammerschmidt, S., et al.** 2005. Illustration of pneumococcal polysaccharide capsule during adherence and invasion of epithelial cells. Infect. Immun. **73:**4653–4667.
32. **Haraldsson, G., W. P. Holbrook, and E. Kononen.** 2004. Clonal similarity of salivary and nasopharyngeal *Fusobacterium nucleatum* infants with actue otitis media experience. J. Med. Microbiol. **53:**161–165.
33. **Heiniger, N., V. Spaniol, R. Troller, M. Vischer, and C. Aebi.** 2007. A reservoir of *Moraxella catarrhalis* in human pharyngeal lymphoid tissue. J. Infect. Dis. **196:**1080–1087.
34. **Hong, W., et al.** 2007. Phosphorylcholine decreases early inflammation and promotes the establishment of stable biofilm communities of nontypeable *Haemophilus influenzae* strain 86-028NP in a chinchilla model of otitis media. Infect. Immun. **75:**958–965.
35. **Hu, F. Z., and G. D. Ehrlich.** 2008. Population-level virulence factors amongst pathogenic bacteria: relation to infection outcome. Future Microbiol. **3:**31–42.
36. **Jurcisek, J. A., et al.** 2007. The PilA protein of non-typeable *Haemophilus influenzae* plays a role in biofilm formation, adherence to epithelial cells and colonization of the mammalian upper respiratory tract. Mol. Microbiol. **65:**1288–1299.
37. **Kadhim, A. L., K. Spilsbury, J. B. Semmens, H. L. Coates, and F. J. Lannigan.** 2007. Adenoidectomy for middle ear effusion: a study of 50,000 children over 24 years. Laryngoscope **117:**427–433.
38. **Kania, R. E., et al.** 2008. Characterization of mucosal biofilms on human adenoid tissues. Laryngoscope **118:**128–134.
39. **Kaplan, C. W., R. Lux, S. K. Haake, and W. Shi.** 2009. The *Fusobacterium nucleatum* outer membrane protein RadD is an arginine inhibitable adhesion required for inter-species adherence and the structured architecture of multispecies biofilm. Mol. Microbiol. **71:**35–47.
40. **Kathju, S., et al.** 2009. Chronic surgical site infection due to suture-associated polymicrobial biofilm. Surg. Infect. **10:**457–461.
41. **Ketterer, M. R., et al.** 1999. Infection of primary human bronchial epithelial cells by *Haemophilus influenzae:* macropinocytosis as a mechanism of airway epithelial cell entry. Infect. Immun. **67:**4161–4170.
42. **Kirketerp-Møller, K., et al.** 2008. Distribution, organization, and ecology of bacteria in chronic wounds. J. Clin. Microbiol. **46:**2717–2722.
43. **Labro, M. T., C. Babin-Chevaye, and M. Mergey.** 2005. Accumulation of azithromycin and roxithromycin in tracheal epithelial fetal cell lines expressing wild type or mutated cystic fibrosis transmembrane conductance regulator protein (CFTR). J. Chemother. **17:**385–392.
44. **Lee, D., and R. M. Rosenfeld.** 1997. Adenoid bacteriology and sinonasal symptoms in children. Otolaryngol. Head Neck Surg. **116:**301–307.
45. **Luke, N. R., J. A. Jurcisek, L. O. Bakaletz, and A. A. Campagnari.** 2007. Contribution of *Moraxella catarrhalis* type IV pili to nasopharyngeal colonization and biofilm formation. Infect. Immun. **75:**5559–5564.
46. **Lysenko, E. S., R. S. Lijek, S. P. Brown, and J. N. Weiser.** 2010. Within-host competition drives selection for the capsule virulence determinant of *Streptococcus pneumoniae*. Curr. Biol. **20:**1222–1226.
47. **May, R. C., and L. M. Machesky.** 2001. Phagocytosis and the actin cytoskeleton. J. Cell Sci. **114:**1061–1077.
48. **McClay, J. E.** 2000. Resistant bacteria in the adenoids: a preliminary report. Arch. Otolaryngol. Head Neck Surg. **126:**625–629.
49. **McClay, J. E.** 2008. Adenoidectomy. eMedicine, Omaha, NB. http://emedicine.medscape.com/article/872216-overview.
50. **Murphy, T. F., L. O. Bakaletz, and P. R. Smeesters.** 2009. Microbial interactions in the respiratory tract. Pediatr. Infect. Dis. J. **28:**S121–126.
51. **Nistico, L., et al.** 2009. Fluorescence "in situ" hybridization for the detection of biofilm in the middle ear and upper respiratory tract mucosa. Methods Mol. Biol. **493:**191–213.
52. **Parsek, M. R., and P. K. Singh.** 2003. Bacterial biofilms: an emerging link to disease pathogenesis. Annu. Rev. Microbiol. **57:**677–701.
53. **Post, J. C., et al.** 1995. Molecular analysis of bacterial pathogens in otitis media with effusion. JAMA **273:**1598–1604.
54. **Pracht, D., et al.** 2005. PavA of *Streptococcus pneumoniae* modulates adherence, invasion, and meningeal inflammation. Infect. Immun. **73:**2680–2689.
55. **Ramadan, H. H., J. A. Sanclement, and J. G. Thomas.** 2005. Chronic rhinosinusitis and biofilms. Otolaryngol. Head Neck Surg. **132:**414–417.
56. **Ratner, A. J., J. L. Aguilar, M. Shchepetov, E. S. Lysenko, and J. N. Weiser.** 2010. Nod1 mediates cytoplasmic sensing of combinations of extracellular bacteria. Cell Microbiol. **9:**1343–1351.
57. **Rayner, M. G., et al.** 1998. Evidence of bacterial metabolic activity in culture-negative otitis media with effusion. JAMA **79:**296–299.
58. **Reid, S. D., et al.** 2009. *Streptococcus pneumoniae* forms surface-attached communities in the middle ear of experimentally infected chinchillas. J. Infect. Dis. **199:**786–794.
59. **Slevogt, H., et al.** 2007. *Moraxella catarrhalis* is internalized in respiratory epithelial cells by a trigger-like mechanism and initiates a TLR2- and partly NOD1-dependent inflammatory immune response. Cell Microbiol. **9:**694–707.
60. **St. Geme, J. W., III.** 2002. Molecular and cellular determinants of non-typeable *Haemophilus influenzae* adherence and invasion. Cell. Microbiol. **4:**191–200.
61. **Stoodley, P., et al.** 2008. Direct demonstration of viable *Staphylococcus aureus* biofilms in an infected total joint arthroplasty: a case report. J. Bone Joint Surg. Am. **90:**1751–1758.
62. **Suzuki, M., T. Watanabe, and G. Mogi.** 1999. Clinical, bacteriological, and histological study of adenoids in children. Am. J. Otolaryngol. **20:**85–90.
63. **Swords, W. E., et al.** 2000. Non-typeable *Haemophilus influenzae* adhere to and invade human bronchial epithelial cells via an interaction of lipooligosaccharide with the PAF receptor. Mol. Microbiol. **37:**13–27.
64. **Thornsberry, C., P. T. Ogilvie, H. P. Holley, Jr., and D. F. Sahm.** 1999. Survey of susceptibilities of *Streptococcus pneumoniae*, *Haemophilus influen-*

zae, and *Moraxella catarrhalis* isolates to 26 antimicrobial agents: a prospective U.S. Study. Antimicrob. Agents Chemother. **43:**2612–2623.
65. **Walters, M. C., III, F. Roe, A. Bugnicourt, M. J. Franklin, and P. S. Stewart.** 2003. Contributions of antibiotic penetration, oxygen limitation, and low metabolic activity to tolerance of *Pseudomonas aeruginosa* biofilms to ciprofloxacin and tobramycin. Antimicrob. Agents Chemother. **47:**317–323.
66. **Weimer, K. E., et al.** 2010. Coinfection with *Haemophilus influenzae* promotes pneumococcal biofilm formation during experimental otitis media and impedes the progression of pneumococcal disease. J. Infect. Dis. **202:**1068–1075.
67. **Winskel, H.** 2006. The effects of an early history of otitis media on children's language and literacy skill development. Br. J. Educ. Psychol. **76:**727–744.
68. **Wright, E. D., A. J. Pearl, and J. J. Manoukian.** 1998. Laterally hypertrophic adenoids as a contributing factor in otitis media. Int. J. Pediatr. Otorhinolaryngol. **45:**207–214.